Industrial Crops & Products 241 (2026) 122768

Contents lists available at ScienceDirect

Industrial Crops & Products

journal homepage: www.elsevier.com/locate/indcrop

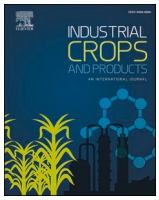

Sustainable microwave-assisted synthesis of high-quality carbon nanotubes from rice husk biochar

Sai Parameshwar [a], Siddharth Jain [b,*], Uday Bhan [a], Varun Pratap Singh [b,c,**]

[a] Department of Petroleum Engineering, UPES, Dehradun, Uttarakhand 248007, India
[b] Department of Mechanical Engineering, UPES, Dehradun, Uttarakhand 248007, India
[c] Solar Thermal Energy Research Group, Mechanical and Mechatronics Engineering Department, Stellenbosch University, 7600, South Africa

ARTICLE INFO

Keywords:
Carbon nanotubes
Biochar
Biomass
Rice husk
Nanotube synthesis
Pyrolysis

ABSTRACT

The conventional synthesis of carbon nanotubes (CNTs) often involves high temperatures, inert atmospheres, non-renewable precursors, and elevated costs. This study explores rice husk, a ligno-cellulose-rich agricultural waste, as a sustainable precursor for CNT synthesis via a two-stage process. First, rice husk was slow pyrolyzed at 300°C, 400°C, and 500°C to produce biochar. The biochar was then reacted with a ferrocene catalyst in varying ratios (1:1, 1:2, and 1:3 ferrocene to biochar, g/g) under microwave irradiation. FESEM analysis revealed highly elongated CNTs with 55 and 78 nm average diameters for biochars pyrolyzed at 400°C and 500°C, respectively. Smaller diameters were observed at higher pyrolysis temperatures and lower ferrocene-to-biochar ratios. Raman spectroscopy confirmed high-quality CNTs ($I_D/I_G < 1$), with the highest degree of wall graphitization ($I_D/I_G = 0.75$) for Rice Husk CNT 500 1:3. Optical studies showed maximum absorbance in the 208–226 nm range, consistent with previous findings. XRD analysis highlighted the influence of amorphous silica in limiting CNT crystallinity at lower pyrolysis temperatures. TEM analysis revealed multiple graphene sheets stacked one above the other, similar to that of Multi-walled carbon nanotubes. This study demonstrates the viability of rice husk as a low-cost, renewable precursor for the synthesis of carbon nanotubes. The findings provide insights into optimizing process parameters for better structural and graphitic properties. By converting agricultural waste into value-added nanomaterials, this work offers a sustainable synthesis of carbon nanotubes using rice husk biochar.

1. Introduction

Carbon Nanotubes are one of the most widely researched nanomaterials as they exhibit properties like high aspect ratio, lightweight, small size, exceptional electro-mechanical properties, and chemical inertness (Norizan et al., 2020; Rathinavel et al., 2021; Shoukat and Khan, 2021). Carbon nanotubes find applications in energy storage, fibres and fabrics, the biomedical industry, drug delivery, water filtration, and thin film electronics (Murjani et al., 2022; Vivanco-Benavides et al., 2022). The commercial methods of carbon nanotube synthesis are Electric arc discharge, Laser ablation, and Chemical Vapor Deposition (CVD) (Rao et al., 2021; Anzar et al., 2020). High thermal energy requirements, exorbitant costs, inert conditions, high impurities, low yield, and dependence on unsustainable precursors are the limitations of the conventional methods of carbon nanotube synthesis (Yahyazadeh et al., 2024; Rao et al., 2021). To solve this issue, environmentally benign and renewable precursors are to be identified and utilized for carbon nanotube synthesis.

According to recent statistics, 998 million tonnes of agricultural waste are produced globally (Thakur et al., 2020), and agricultural and allied activities account for 24 % of global greenhouse gas emissions (Ranguwal et al., 2023). The burning of agricultural crop waste results in undesirable emissions of greenhouse gases and depletes soil fertility. Additionally, frequent burning of agricultural waste releases smog, which degrades the quality of atmospheric air and adversely affects human health (Divyabharathi et al., 2024; Shukla et al., 2022). An effective solution to this problem is the conversion of agricultural waste into value-added products by-effective conversion processes. Agricultural waste is often used as a feedstock for the production of bioethanol, biochar, and other sustainable, environmentally friendly products. Agricultural waste has the potential to be a renewable, abundant, cost-effective, and environmentally friendly precursor for carbon nanotube synthesis.

* Corresponding author.
** Corresponding author at: Department of Mechanical Engineering, UPES, Dehradun, Uttarakhand 248007, India.
E-mail addresses: siddharth.jain@ddn.upes.ac.in (S. Jain), vpsingh@sun.ac.za (V.P. Singh).

https://doi.org/10.1016/j.indcrop.2026.122768
Received 18 February 2025; Received in revised form 20 January 2026; Accepted 23 January 2026
Available online 3 February 2026

Nomenclature

eV	Electron Volt
Nm	Nano metres
μm	Micrometres
Mm	Milli meters
I_D	Intensity of D-band
I_G	Intensity of G-band
Ghz	Giga-hertz
Cp	Centi-poise
g/cc	Gram per cubic centimetre
kW	Kilo-Watt
Rpm	Revolutions per minute
g	Gram
g/g	Gram per Gram
μ	Micron
%wt.	Percentage weight
ʎ	X-ray wavelength
Θ	Braggs angle
N	Order of Reflection
D	Inter-planar spacing
E_{in}	Energy Input
Q_{HHV}	Energy contained in solid biomass
Q_s	Energy required to heat and convert biomass to pyrolysis product
m_{feed}	Mass of feedstock
c_p	Specific heat capacity of biomass
T_P	Pyrolysis temperature
~	Approximately

Abbreviations

ASTM	American Society for Testing and Materials
CHNS	Carbon Hydrogen Nitrogen Sulphur
CNT	Carbon Nanotubes
RHCNT	Rice husk derived Carbon nanotubes
RHCNT 300	Rice husk synthesized from biochar pyrolyzed at 300ºC
RHCNT 400	Rice husk synthesized from biochar pyrolyzed at 400ºC
RHCNT 500	Rice husk synthesized from biochar pyrolyzed at 500ºC
CNT 500 1:1	Carbon nanotubes synthesized with rice husk pyrolyzed at 500ºC with 1:1 wt ratio of ferrocene and rice husk biochar respectively.
CNT 500 1:2	Carbon nanotubes synthesized with rice husk pyrolyzed at 500ºC with 1:2 wt ratio of ferrocene and rice husk biochar respectively.
CNT 500 1:3	Carbon nanotubes synthesized with rice husk pyrolyzed at 500ºC with 1:3 wt ratio of ferrocene and rice husk biochar respectively.
CNT 400 1:1	Carbon nanotubes synthesized with rice husk pyrolyzed at 400ºC with 1:1 wt ratio of ferrocene and rice husk biochar respectively.
CNT 400 1:2	Carbon nanotubes synthesized with rice husk pyrolyzed at 400ºC with 1:2 wt ratio of ferrocene and rice husk biochar respectively.
CNT 400 1:3	Carbon nanotubes synthesized with rice husk pyrolyzed at 400ºC with 1:3 wt ratio of ferrocene and rice husk biochar respectively.
CNT 300 1:1	Carbon nanotubes synthesized with rice husk pyrolyzed at 300ºC with 1:1 wt ratio of ferrocene and rice husk biochar respectively.
CNT 300 1:2	Carbon nanotubes synthesized with rice husk pyrolyzed at 300ºC with 1:2 wt ratio of ferrocene and rice husk biochar respectively.
CNT 300 1:3	Carbon nanotubes synthesized with rice husk pyrolyzed at 300ºC with 1:3 wt ratio of ferrocene and rice husk biochar respectively.
CVD	Chemical Vapor Deposition
DCM	Dichloro Methane
DTGS	Deuterated triglycine sulphate
FESEM	Field Emission Scanning Electron Microscopy
FTIR	Fourier Transform Infrared spectroscopy
XRD	X-ray Diffraction
TEM	Transmission Electron Microscopy
VM	Volatile Matter
HHV	Higher Heating Value
FC	Fixed Carbon
AC	Ash Content
Fe	Iron
NP	Nanoparticles
LCA	Life Cycle Assessment
α-Fe_2O_3	Hematite,
Fe_3C	Cementite
Fe_3O_4	Magnetite
JCPDS	Joint Committee on Powder Diffraction Standards

Pyrolysis is defined as the thermal decomposition of biomass in inert or vacuum conditions to obtain products like pyrolysis gas, bio-oil, and biochar (Zha et al., 2023). The three types of pyrolysis are slow, fast, and flash pyrolysis. Slow pyrolysis is characterized by high residence times (5–30 min) and lower temperature rates (300–700°C) (Pielsticker et al., 2021). Fast pyrolysisis the rapid thermal decomposition of biomass at very high temperatures (400–800°C) and shorter residence time (<2 s) compared to slow pyrolysis. In flash pyrolysis, the temperature may spikeup to 2500°C for a very short interval of time (<0.5 s) (Sekar et al., 2021; Ighalo et al., 2022). (Baghel and Kaushal, 2022) reported the carbon nanotube synthesis from *Prosopis juliflora* biochar under microwave irradiation conditions. The carbon nanotubes of size ranging from 10 to 60 nm were synthesized from *Prosopis juliflora* biochar precursor. Hidalgo et al. (2019) synthesized carbon nanotubes having a diameter of 17–100 nm from four different biochar precursors. Super long (0.7–2 mm) carbon nanotubes were synthesized from cellulose extracted from Palm kernel shells by microwave pyrolysis synthesis by EsoheOmoriyekomwan et al. (2022). The highest quality of carbon nanotubes was obtained after microwave treatment at 1400°C (I_D/I_G=0.84). Biochar obtained by pyrolysis of three different species of algae, namely, *Scenedesmusalmeriensis, Macrocystispyrifera,* and *Sarcothalia crispate* was used for carbon nanotube synthesis by Hidalgo et al. (2023). Higher carbon content was observed for carbon nanotubes synthesized from *Scenedesmus almeriensis* microalgae biochar. Le et al. (2021) synthesized carbon nanotubes by co-pyrolysis of eucalyptus oil and ferrocene catalyst at a temperature range of 800–900°C. The highest carbon nanotube yield of 45 % was obtained at 850°C with a 1:1 molar ratio of eucalyptus oil to ferrocene.

Microwave is a form of electromagnetic energy that has a frequency and wavelength of 0.3–300Ghz and 1mm-1m respectively (Rifna et al., 2019). Microwave-assisted heating is an effective method compared to conventional heating methods due to its faster heating rates and lower energy requirements. Microwave energy works with the principle of localized heating, where the microwave energy interacts with the reactant particles at the molecular level, which makes the heating process expeditious (Palma et al., 2020; Kumar et al., 2020). Also, microwave heating is characterized by volumetric heating, where the heat and mass transfer occur in the same direction (Bajpai and Wagner, 2015; Mao et al., 2021). The microwave-assisted method is an energy-efficient, time-saving, and effective method that can be used for the synthesis of

carbon nanotubes.

Rice husk is an abundant, cheap agricultural waste, environmentally benign source of biomass. The excessive charring of waste rice husk in farmlands releases toxic smoke into the atmosphere, leading to environmental damage and health issues (Quispe et al., 2017; Pode, 2016). The presence of organic carbon and silica in rice husk makes it a suitable raw material for numerous applications like construction, fertilizers, and fuel (Shamsollahi and Partovinia, 2019; Kordi et al., 2024). In this study, we propose another application of waste rice husk as a feedstock in the synthesis of carbon nanotubes by a two-step conversion process. The slow pyrolysis of waste rice husk sample was done to obtain carbonaceous, amorphous biochar at three different pyrolysis temperatures 300, 400, and 500°C. The second step involves the conversion of biochar to carbon nanotubes under microwave irradiation conditions in the presence of the organometallic compound, ferrocene as the catalyst. Also the effect of the ratio of rice husk biochar to the organometallic catalyst, ferrocene, on the characteristics, yield and the quality of carbon nanotubes is hardly investigated till now. The rice husk biochar precursors (pyrolyzed at three different temperatures, 300, 400, and 500°C) are individually treated with three different ratios (g/g) of ferrocene to rice husk biochar(1:1, 1:2, 1:3) in the presence of microwave energy to synthesize the desired carbon nanotubes. Further, the synthesized rice husk carbon nanotubes are characterized by various analysis techniques, namely, X-ray diffraction, Fourier transform Infrared spectroscopy, Raman spectroscopy, Particle size analysis by dynamic light scattering, Ultra-violet spectroscopy, TEM analysis and Finite-element scanning electron microscopy.

2. Materials and experimental method

A 27-liter, 900-watt power, Panasonic NN-CT644M model microwave oven was used as the microwave irradiation source for this study. The organometallic compound, Ferrocene was purchased from Doon Chemicals, Dehradun, India. The agricultural waste rice husk was sourced from a local agricultural field in Dehradun, India.The rice husk sample was initially open-air dried for two days, then pulverized toa fine powder using an electric mixer andfurther sieved with a 75 μm mesh to get the required powder sample for pyrolysis. A detailed diagram of the two-step process of conversion of waste rice husk to carbon nanotubes is shown in Fig. 1.

2.1. Slow pyrolysis of agricultural waste to produce biochar

A 100 g sample of powdered rice husk was placed in the fixed-bed pyrolysis reactor, and a slow pyrolysis process was performed at 300, 400, and 500°C for a residence time of 3 h. The desired pyrolysis temperature was attained by slowly ramping the reactor temperature at 10°C/minute. After completing the process, the sample was allowed to cool down and thenremoved from the chamber. The biochar yield after the slow-pyrolysis process is given by the following equation:

$$\text{Biochar yield}(\%) = \frac{(\text{Weight of biochar in grams})}{(\text{Weight of rice husk in grams})} \times 100 \quad (1)$$

2.2. Rice husk Carbon nanotube synthesis

A total of nine ferrocene to rice husk biochar mixture samples were prepared for the carbon nanotube synthesis by separately mixing the rice husk biochar that had been pyrolyzed at 300, 400, and 500°C with ferrocene at three distinct ferrocenes to biochar ratios (gram/gram): 1:1, 1:2, and 1:3, respectively. Each sample of the ferrocene-to-biochar combination was separately transferred to a 30-milliliter glass vial

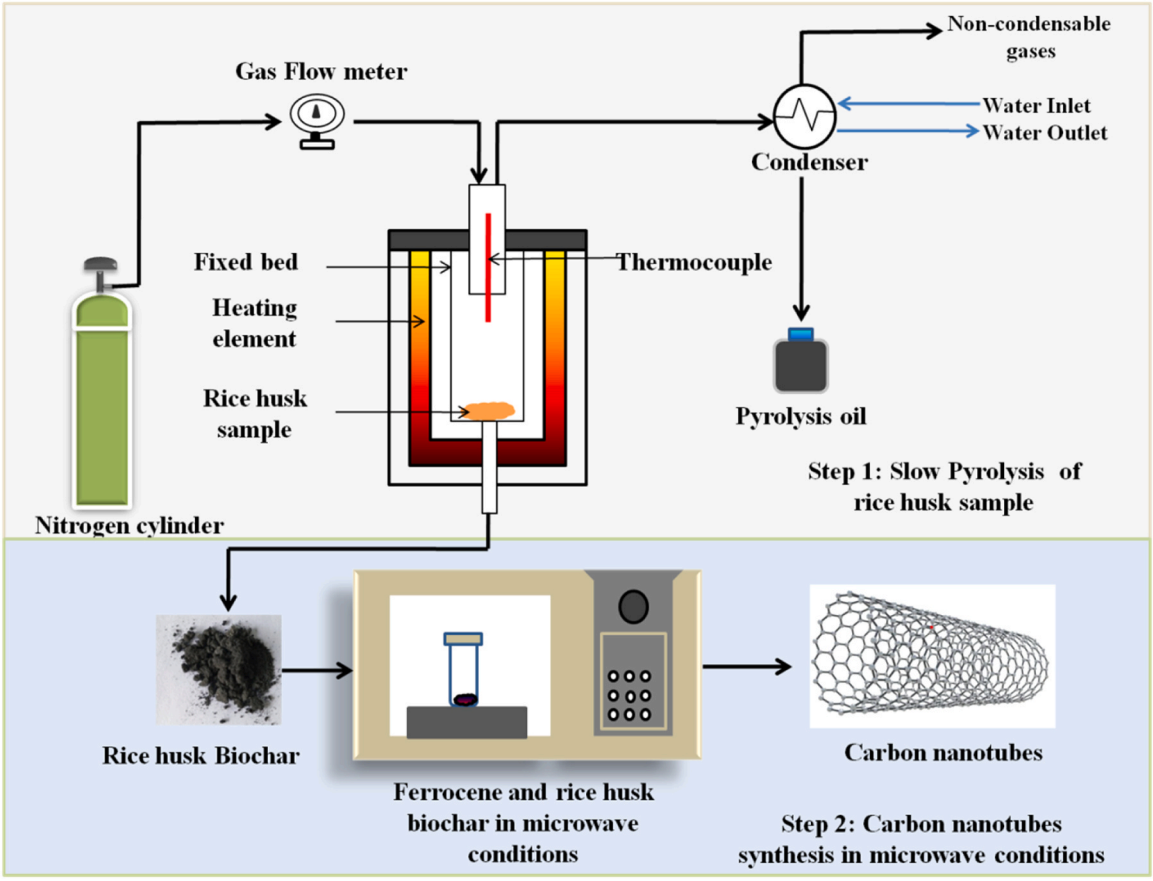

Fig. 1. Two-step process of conversion of waste rice husk to carbon nanotubes.

before being put in the microwave oven to synthesize carbon nanotubes. The microwave temperature was maintained at 120°C for 15 min. The reaction commenced within a few seconds as ferrocene decomposed into cyclopentadienyl (C_5H_5) and free iron atoms. Upon condensation and aggregation, free iron particles are converted to iron nanoparticles, and they are scattered on the surface of rice husk biochar. Iron nanoparticles act as catalysts in this carbon nanotube synthesis under microwave irradiation. Once the reaction is completed, the set-up is allowed to cool, and the glass vial is removed from the oven. It was observed that extremely fine carbon nanotube particles adhered along the walls of the glass vial. The carbon nanotubes were carefully removed and sent for further characterization. The two-step process of conversion of rice husk to carbon nanotubes is depicted in Fig. 1.

2.3. Characterization of rice husk biochar and carbon nanotubes

Rice husk biochar was characterized by proximate analysis and ultimate analysis methods. The proximate analysis for moisture, ash, and volatile content was performed using the ASTM D3173, D3175, and E1755 methods, respectively. The fixed carbon (%) was calculated as per the following equation:

Fixed carbon(%)= [100-(Ash content (%)+Volatile content(%)+Moisture content(%))] (2)

Also, the ultimate (CHNS) analysis of rice husk biochar was done using a EuroEA CHNS analyzer, the H/C molar ratio and O/C molar ratio were evaluated based on the results obtained from the ultimate analysis of rice husk biochar.The X-ray diffraction analysis of rice husk carbon nanotubes was performed using the Bruker D8 Advance Eco model, having a 1 kW X-ray source with a vertical, θ/2θ geometry. The Fourier transform infrared (FTIR) spectroscopy helps to identify the functional groups, and chemical bonds in both organic and inorganic compounds by evaluating the absorption of infrared radiation in a wide range of wavelengths. For this study, the Perkin Elmer Frontier FT-IR/FIR model was used with a Deuterated Triglycine Sulphate (DTGS) detector. The particle size distribution of rice husk-synthesized carbon nanotubes was evaluated by dynamic light scattering technique. Malvern ZEN 1690 (S-type) model was used for dynamic light scattering studies with a measurement range of 0.3 nm to 5 microns. The rice husk carbon nanotube particles were suspended in the Dichloromethane (DCM) solution having the viscosity, refractive index, dielectric constant, and density of 0.413 cp, 1.4125, 8.93, and 1.318 g/cc, respectively. The DCM solution along with suspended carbon nanotube particles was initially sonicated for 45 min, followed by centrifuging it for 30 min at 3300 rpm. The heavier carbon nanotube particles agglomerate and settle at the bottom of the centrifuge tube. The supernatant liquid was carefully transferred to the glass cuvette for dynamic light scattering analysis.

Ultraviolet spectrometry is an effective, non-destructive analytical method used for organic and some inorganic compounds to measure the absorbance or emittance of ultra-violet or visible light rays through a sample in comparison to a reference sample. The rice husk carbon nanotube solutions wereinitially dispersed in the Dichloromethane solution and then sonicated in a Branson 3800 model ultrasonic bath at 35 Hz for 45 min. The agglomeration of the carbon nanotube particles due to van der Waals forces of attraction can be effectively separated by the sonication process. The sonicated sample was allowed to rest for 2 h, and some agglomerated carbon nanotube particles settled at the bottom. The supernatant sample was carefully transferred to a 10 mm,3.5 ml quartz cuvette, and placed inside a Shimadzu UV-1900I model ultraviolet spectrometer for analysis. The wavelength for the ultraviolet spectrometry analysis was set in the range of 200–1000 nm.The Raman spectroscopy analysis was performed with the RIMS-U-DC model having a laser power and wavelength of 300 milli Volts and 532 nm respectively. FEI Apreo LoVac (1.5–2 nm resolution and magnifications of 10x-300000x) was used to evaluate the surface morphology of the synthesized carbon nanotubes.

3. Result and discussion

This section presents the results from the characterization of rice husk biochar and the subsequent synthesis of carbon nanotubes (CNTs). The effects of varying pyrolysis temperatures (300°C, 400°C, and 500°C) and the ferrocene-to-biochar ratios (1:1, 1:2, and 1:3) on the properties of biochar and CNTs are discussed. Characterization techniques such as proximate and ultimate analysis, X-ray diffraction (XRD), Fourier transform infrared spectroscopy (FTIR), and dynamic light scattering (DLS) were employed to assess the quality, structural changes, and particle size distribution of the products.

3.1. Characterization of rice husk biochar precursor

The slow pyrolysis of rice husk, an agricultural waste, was performed at temperatures of 300°C, 400°C, and 500°C. The results showed a noticeable reduction in biochar yield with increasing pyrolysis temperature due to a higher degree of thermal decomposition. Specifically, at 300°C, the biochar yield was 44.53 ± 3.32 %, but this decreased to 40.6 ± 1.927 % at 400°C and further to 35.02 ± 1.81 % at 500°C. This reduction in yield can be attributed to the higher rate of thermal decomposition of lignocellulose biomass as the temperature increases. The proximate analysis revealed a decrease in moisture and volatile content as the pyrolysis temperature increased from 300°C to 500°C. In contrast, both ash and fixed carbon content increased with higher pyrolysis temperatures. The ultimate analysis confirmed that carbon is the major constituent of the rice husk, and the carbon content increased with the rising pyrolysis temperature. The H/C and O/C molar ratios decreased with increasing temperature, indicating improved aromaticity and reduced hydrophilicity of the rice husk biochar. The detailed results of biochar yield, proximate, and ultimate analyses are shown below:

At 300°C, the biochar yield was 44.53 %, with 4.92 % moisture, 39.13 % volatile matter, 4.30 % ash, and 51.65 % fixed carbon. The carbon content (C) was 40.76 %, hydrogen (H) was 2.62 %, and oxygen (O) was 56.42 %. At 400°C, the biochar yield decreased to 40.67 %, with 3.31 % moisture, 36.28 % volatile matter, 4.98 % ash, and 55.43 % fixed carbon. The carbon content increased to 44.73 %, with hydrogen (H) at 2.06 % and oxygen (O) at 53.05 %. At 500°C, the biochar yields further decreased to 35.02 %, with moisture at 2.36 %, volatile matter at 31.67 %, ash at 5.47 %, and fixed carbon at 60.50 %. The carbon content increased to 50.48 %, hydrogen (H) to 1.12 %, and oxygen (O) to 48.29 %. The H/C and O/C molar ratios also decreased progressively with increasing temperature, indicating improvements in biochar's structural properties and aromaticity. The H/C and O/C molar ratios decrease with increasing pyrolysis temperature, as shown in Table 1. Lower H/C and O/C molar ratios indicate better aromaticity and lower hydrophilicity, respectively, in rice husk biochar.

3.2. X-ray diffraction (XRD) analysis of Rice husk biochar and Carbon nanotubes

The results of X-ray diffraction (XRD) analysis performed for rice husk biochar and rice-husk-derived carbon nanotubes are depicted in Fig. 2 (a) and (b), respectively. The peaks for rice husk biochar at 300, 400, and 500°C were observed at 21.88, 22.07, and 21.64°, respectively, all of which lie on the (002) plane. The prominent peak of rice husk biochar indicates the presence of amorphous silica, which is a principal constituent of rice husk (Islam et al., 2021). As the temperature increases from 300 to 500°C, the crystalline nature of the rice husk biochar improves as the major peak at 21.64–22.07° becomes narrower. This indicates that the major constituent of the rice husk sample, amorphous silica, gradually crystallizes with increasing pyrolysis temperature. The XRD of rice husk biochar is shown in Fig. 2(a) and the results agree with

Table 1
The results of the proximate and ultimate analysis of rice husk biochar.

Pyrolysis Temperature (°C)	Proximate analysis				Ultimate analysis						
	Moisture (%)	Volatile matter (%)	Ash content (%)	Fixed carbon (%)	C(%)	H (%)	N (%)	S (%)	O(%)	H/C molar ratio	O/C molar ratio
Room temp.	8.90	58.48	0.28	32.26	31.51	3.94	0.00	0.00	64.55	1.50	0.77
300	4.92	39.13	4.30	51.65	40.76	2.62	0.22	0.00	56.42	0.83	0.52
400	3.31	36.28	4.98	55.43	44.73	2.06	0.16	0.00	53.05	0.59	0.44
500	2.36	31.67	5.47	60.50	50.48	1.12	0.11	0.00	48.29	0.24	0.36

the works of literature we studied (Islam et al., 2021; Armynah et al., 2018).

In the case of rice husk carbon nanotubes pyrolyzed at 300,400 and 500°C, the common and the most prominent peak lies in the highly ordered graphite (002) plane. The graphite (002) plane has an interplanar spacing of 0.31 nm, which corresponds to the interplanar spacing value of multi-walled carbon nanotubes . The sharpness of the peak in the graphite (002) plane of rice husk-derived carbon nanotubes indicates the presence of multi-walled carbon nanotubes. Another common peak for all synthesized carbon nanotubes was around 43.1° and it corresponds to the graphite (100) plane, which is also mostly observed in carbon nanotubes (Kim et al., 2012). While comparing the XRD analysis of rice husk biochar and rice husk carbon nanotubes, it is evident that the synthesized carbon nanotubes have become more crystalline indicated by a sharp and prominent peak seen in the graphite (002) plane. Moreover, when the ferrocene to biocharratio is varied from 1:1–1:3, there is a reduction in the sharpness of the graphite crystal (002) plane, possibly due to the presence of amorphous silica in rice husk biochar. The XRD curve of Rice husk CNT 300 1:3 and Rice husk CNT 300 1:2 exhibited a broad peak at 22.2°, which is associated with amorphous silica present in rice husk biochar pyrolyzed at 300°C as shown in Fig. 2**(b)**. In other words, the crystallinity of the graphite (002) plane is reduced due to the presence of amorphous silica in rice husk biochar. This is confirmed by the high silicon content detected by the EDX spectrum of RH CNT 300 1:3. In addition to the above-mentioned prominent peaks, minor diffraction peaks associated with Fe-based phases were observed. The peak at ~36° (2θ) corresponds to the (311) plane of Fe_3O_4 (JCPDS PDF 19–0629) (Namikuchi et al., 2021), indicating partial oxidation of the Fe catalyst. The peaks at ~39.5° and ~47° are indexed to the (121) and (211) planes of Fe_3C (JCPDS PDF 35–0772) (Chen et al., 2019), confirming iron carbide formation during CNT growth. A weak peak at approximately 48.6° is primarily attributed to α-Fe_2O_3 (024) (JCPDS PDF 33–0664) (Liu et al., 2020; Baghel et al., 2022). As per EDX spectrum of RHCNT 300 1:3 shown in Fig. 2**(c)**, the silicon content of 14.19 ± 0.15 %wt. was estimated. Some of the previous research also confirmed the presence of a broad peak at approximately 22° for rice husk biochar due to its inherent silica content (Burachevskaya et al., 2023; Yang et al., 2023). The peak adjacent to the Si Kα signal corresponds to the Si Kβ transition (~1.84 keV), while minor peaks at ~0.7, 6.4, and 7.1 keV are attributed to Fe Lα, Fe Kα, and Fe Kβ emissions, respectively.

The inter-planar spacing (ᴅ-spacing) of CNTs can be determined by Bragg's Law as follows:

$$n^*\lambda = 2^*d^*\sin\theta \quad (3)$$

where, n is the order of reflection, λ is the wavelength of X-rays (0.154 nm), d is the inter-planar spacing, and θ is the Braggs angle (Wei and Li, 2016). The inter-planar spacing of the (002) peak was calculated as 0.314 nm, which corresponds to inter-planar spacing range (0.31–0.35 nm) of MWCNTs (Kharissova and Kharisov, 2014; Hassan, 2015).

3.3. Fourier Transform Infrared (FTIR) Spectroscopy

The FTIR spectrometry results of RHCNTs pyrolyzed at 300,400 and 500°C are shown in Fig. 3(a), (b), and (c), respectively. A common, broad peak was observed for rice husk carbon nanotubes in the wave number ranges of 1091–1109 cm^{-1} and it can be attributed to C—O symmetric stretching seen in alcohols. Also, all the rice husk carbon nanotubes exhibit two minor peaks at 1416–1434 cm^{-1}and1598–1628 cm^{-1}. The presence of aromatics, such as esters and phenols, contributes to the peak at 1416–1434 cm-1, which corresponds to C—C stretching. The 1598–1628 cm-1 peak is due to C═C asymmetric stretching by aromatic groups that are present in lignin, and it represents sp^2 hybridized (G-band) carbon atoms. Another common broad peak was observed at approximately 3400 cm^{-1}, which is due to the presence of O—H stretching. A weak peak was observed at 2918–2926 cm^{-1} for rice husk carbon nanotubes pyrolyzed at 500°C, as depicted in Fig. 3**(c)**. The weak peak at 2918–2926 cm^{-1} can be associated with symmetric and asymmetric C—H stretching.

3.4. Dynamic Light Scattering (DLS) analysis for particle size distribution

The hydrodynamic diameter of the synthesized rice husk carbon nanotubes was found to be influenced by both the ferrocene-to-biochar ratio and the pyrolysis temperature. The most minor hydrodynamic diameter of 140 nm was recorded for RHCNT 500 1:1. As the ferrocene to biochar ratio increased from 1:1–1:3, the hydrodynamic diameter of the carbon nanotubes also increased. This trend indicates that a higher ferrocene ratio leads to larger particle sizes in the synthesized nanotubes.

As the pyrolysis temperature decreased from 500°C to 300°C, the hydrodynamic diameter of the carbon nanotubes also increased, irrespective of the ferrocene to biochar ratio. This observation aligns with findings by (Hidalgo et al., 2019), who reported that carbon nanotubes made from biochar pyrolyzed at 600°C had a smaller hydrodynamic diameter than those made from biochar pyrolyzed at 400°C (Hidalgo et al., 2019).

The particle size of the biochar precursor, which is a crucial factor in the synthesis of carbon nanotubes, was measured for rice husk biochar pyrolyzed at 500°C, 400°C, and 300°C. The average particle sizes were determined to be 18.5 ± 0.4 μm at 500°C, 26.4 ± 0.5 μm at 400°C, and 32.9 ± 0.4 μm at 300°C. The larger particle size of rice husk biochar pyrolyzed at 300°C may have contributed to the higher hydrodynamic diameter observed for RHCNT 300 across various ferrocene-to-biochar ratios. These findings align with those of (Hidalgo et al., 2019), who reported that an increase in the particle size of the biochar precursor can increase the size of the synthesized carbon nanotubes. The hydrodynamic diameters of the synthesized rice husk carbon nanotubes for each ferrocene to biochar ratio were as follows: For RHCNT 500 1:1, the hydrodynamic diameter was 140 nm; for RHCNT 500 1:2, the hydrodynamic diameter increased to 180 nm; and for RHCNT 500 1:3, the hydrodynamic diameter was 187 nm. For RHCNT 400 1:1, the hydrodynamic diameter was 196 nm, and for RHCNT 400 1:2, it increased to 227 nm. When the ratio was 1:3, the hydrodynamic diameter was 236 nm. For RHCNT 300 1:1, the diameter was 254 nm; it increased to 280 nm for a 1:2 ratio and to 322 nm for a 1:3 ratio.

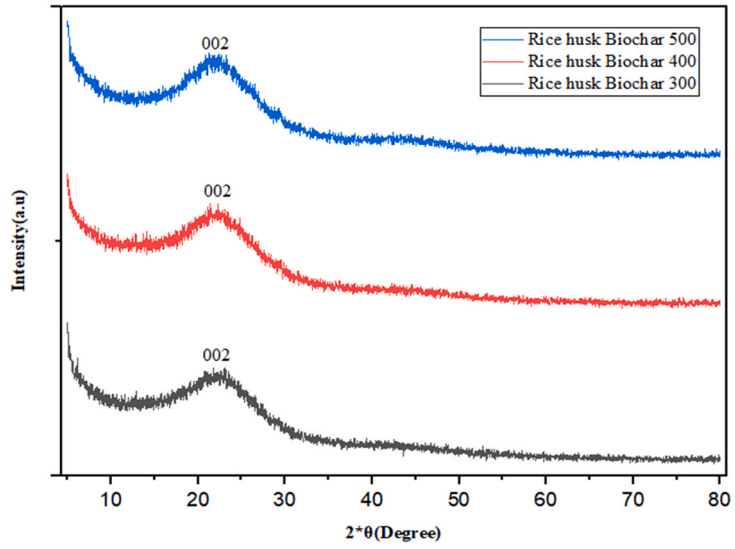

(a)

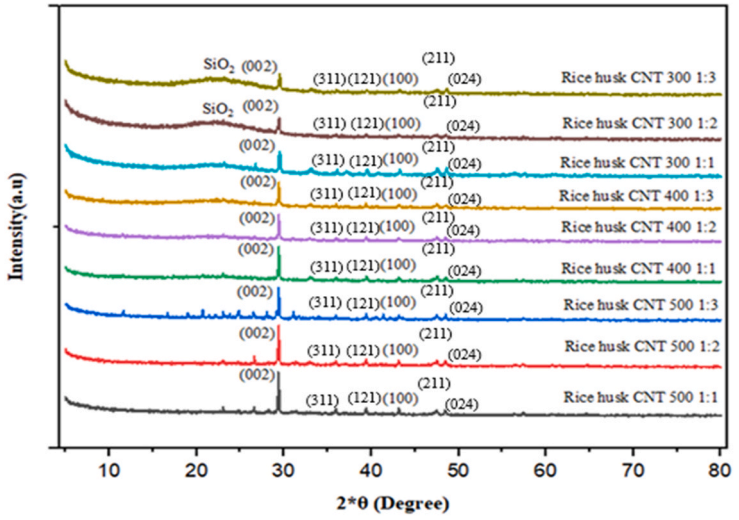

(b)

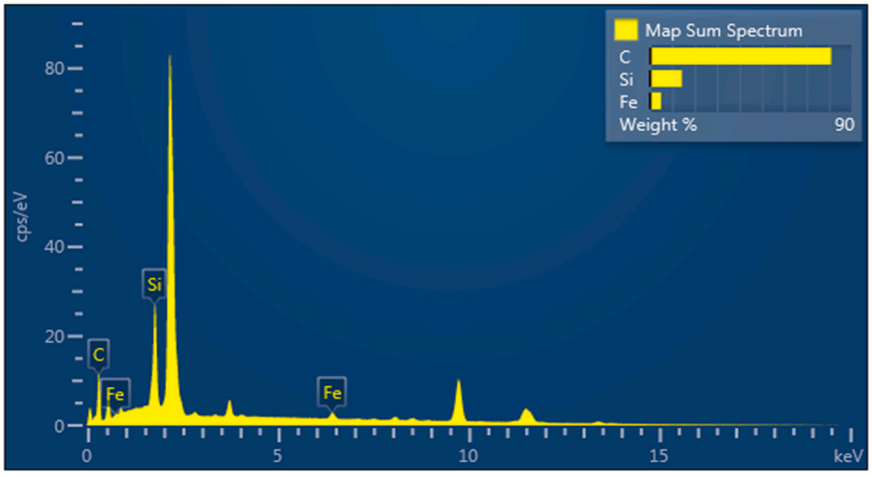

(c)

Fig. 2. (a) XRD results of RHBC 300, RHBC 400, and RHBC 500, (b) XRD results of RHCNTs, (c) EDX spectrum of RHCNT 300 1:3.

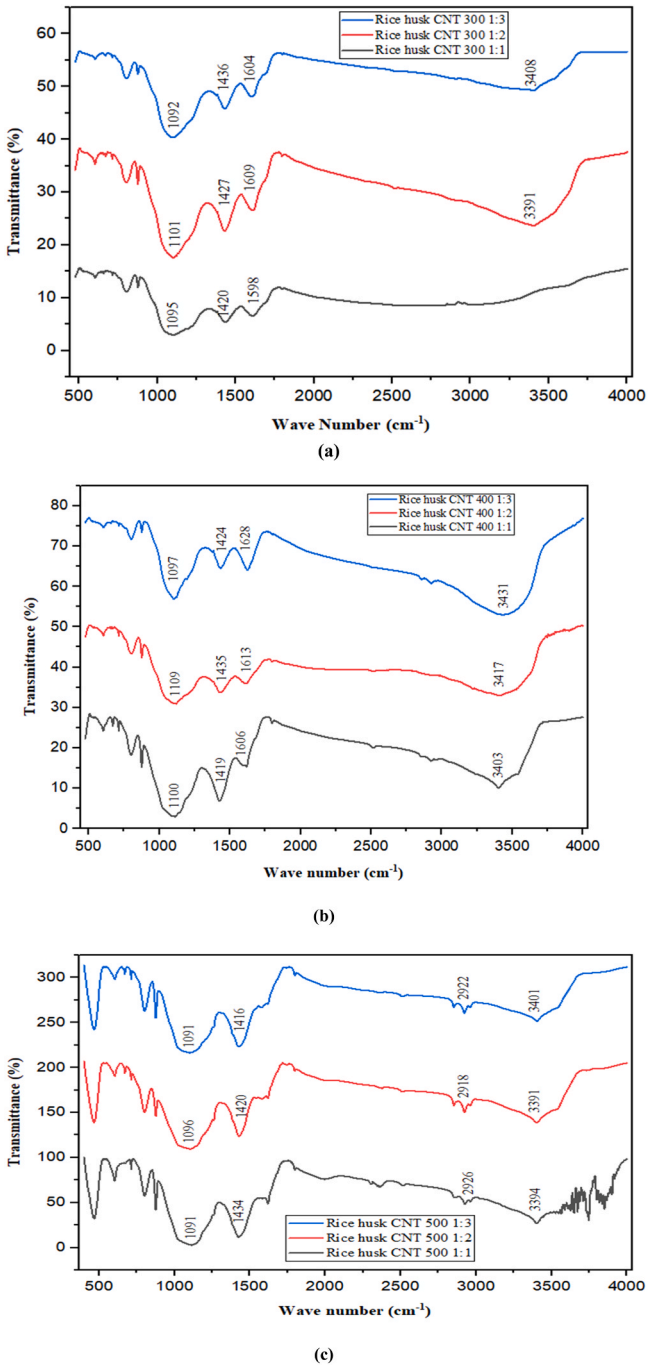

Fig. 3. (a) FTIR results of RHCNT 300 1:1, RHCNT 300 1:2, and RHCNT 300 1:3, (b) FTIR results of RHCNT 400 1:1, RHCNT 400 1:2, and RHCNT 400 1:3, and (c) FTIR results of RHCNT 500 1:1, RHCNT 500 1:2, and RHCNT 500 1:3.

3.5. Ultraviolet Spectrometry

The ultraviolet spectrometry analysis of rice husk carbon nanotubes synthesized at different pyrolysis temperatures and ferrocene to biochar ratios revealed maximum ultraviolet absorption in the range of 208–226 nm. The maximum absorbance of rice husk carbon nanotubes was observed in this ultraviolet spectrum, and it gradually decreased in the infrared region. The energy band gap corresponding to the maximum ultraviolet absorption of the synthesized rice husk carbon nanotubes ranged from 5.48 to 5.96 eV. The highest energy band gap of 5.96 eV was observed for RHCNT 500 1:1, while the lowest value of 5.48 eV was observed for RHCNT 300 1:1. These findings are consistent with previous studies, such as (Algadri et al., 2017), who reported an energy band gap of 5.69–5.84 eV for carbon nanotubes (Algadri et al., 2017). According to Singh et al. (2018), the energy band gap is inversely proportional to the particle size of the material, and this was observed in the current study, where the smallest particle size corresponded to the highest energy band gap, and the largest particle size corresponded to the lowest energy band gap (Singh et al., 2018). Collins et al. (2001) also reported that smaller carbon nanotube shells tend to exhibit higher energy band gaps, which is reflected in the results for RHCNT 500 1:1 and RHCNT 300 1:1, which exhibited the smallest and largest particle sizes, respectively (Collins et al., 2001).

The wavelength of maximum absorbance and the energy band gaps for each rice husk carbon nanotube sample are as follows: For RHCNT 500 1:1, the wavelength of maximum absorbance was 208 nm, and the energy band gap was 5.96 eV; for RHCNT 500 1:2, the wavelength was 224 nm, and the energy band gap was 5.53 eV; for RHCNT 500 1:3, the wavelength was 214 nm, and the energy band gap was 5.79 eV. For RHCNT 400 1:1, the wavelength was 210 nm, and the energy band gap was 5.90 eV; for RHCNT 400 1:2, the wavelength was 220 nm, and the energy band gap was 5.64 eV; for RHCNT 400 1:3, the wavelength was 225 nm, and the energy band gap was 5.51 eV. For RHCNT 300 1:1, the wavelength was 226 nm, and the energy band gap was 5.48 eV; for RHCNT 300 1:2, the wavelength was 223 nm, and the energy band gap was 5.56 eV; for RHCNT 300 1:3, the wavelength was 217 nm, and the energy band gap was 5.71 eV (Fig. 4).

3.6. Raman Spectroscopy

The Raman spectroscopy analysis of rice husk carbon nanotubes revealed distinct band peaks at 1350 cm^{-1} and 1593 cm^{-1} , corresponding to the D-band (D-mode) and G-band (G-mode), respectively. The G-band, attributed to C—C stretching in graphitic materials, signifies the presence of sp^2 hybridized carbon atoms, while the D-band corresponds to sp^3 hybridization and indicates structural defects in the carbon nanotubes. Raman spectra of RHCNT 500, RHCNT 300 and RHCNT 400 are shown in Fig. 5(a), Fig. 5(b) and Fig. 5(c), respectively.

A broad peak at 2750 cm^{-1} , referred to as the 2D-band, was also observed, which is typically associated with the overtone of the G-band. The lower intensity of the 2D band suggests the presence of multi-walled carbon nanotubes, a characteristic feature linked to a higher number of layers in the carbon material, as reported by Hossain et al. (2016), The 2D-band was more prominent in RHCNT 500 1:3, followed by RHCNT 500 1:2.

In Raman spectroscopy, the intensity ratio of the D-band (I_D) to the G-band (I_G) provides insight into the quality of the carbon nanotubes

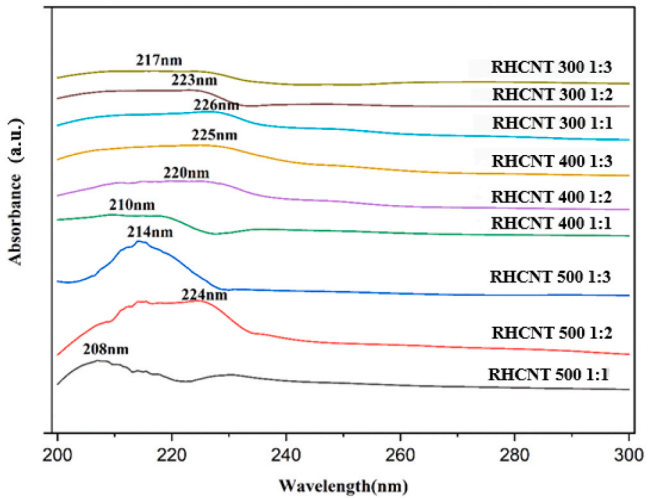

Fig. 4. Ultraviolet absorption spectra of rice husk carbon nanotubes.

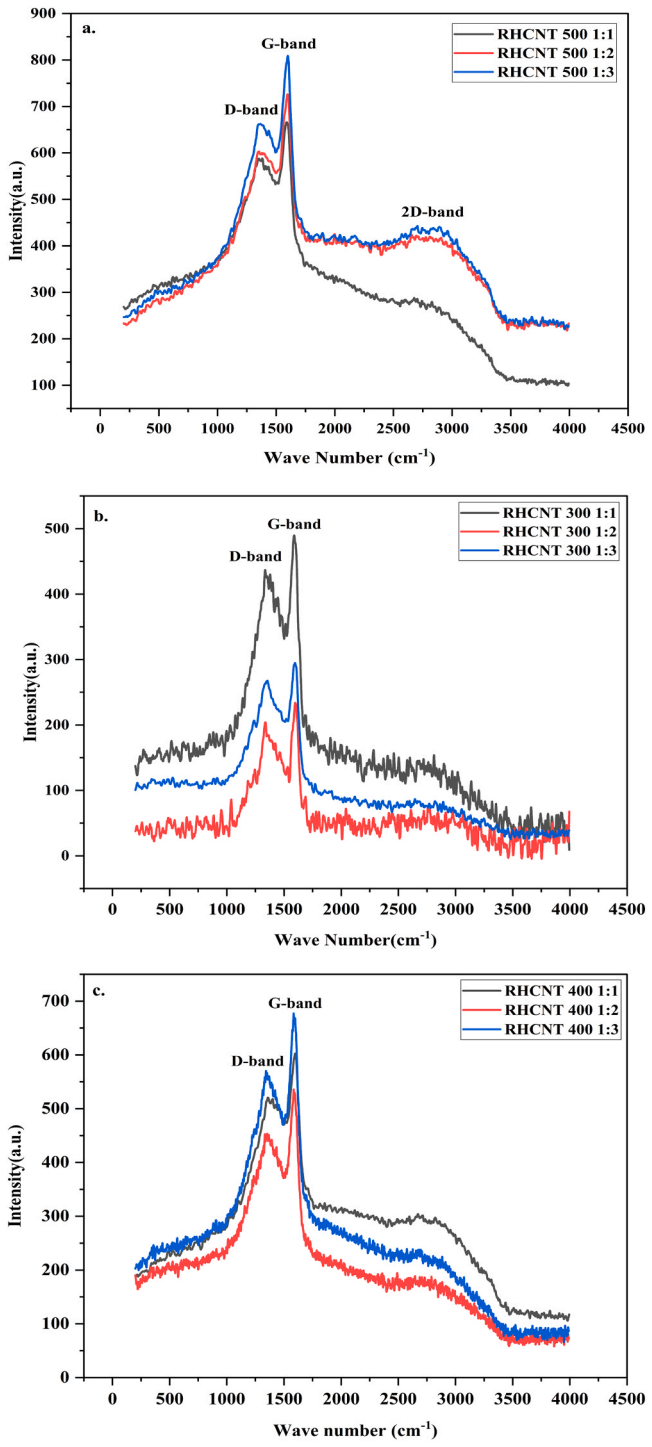

Fig. 5. Raman spectra of a) RHCNT 500, b) RHCNT 300 and c) RHCNT 400.

and the degree of wall graphitization. A lower ID/IG ratio indicates better quality and a higher degree of wall graphitization. The I_D/I_G ratios for the rice husk-derived carbon nanotubes, presented below, were relatively low, all falling below 1, indicating a high degree of graphitization in the materials. (Baghel 7 Kaushal, 2022) also used biochar that was pyrolyzed at 300, 400, 500, and 600°C to report an I_D/I_G value < 1 for *Prosopis* Juli Flora carbon nanotubes. The lowest I_D/I_G ratio of 0.75 was observed for RHCNT 500 1:3, suggesting a high degree of wall graphitization and superior quality of the carbon nanotubes. For both RHCNT 500 and RHCNT 400, the I_D/I_G ratio decreased as the ferrocene to biochar ratio increased from 1:1–1:3. For RHCNT 300, the I_D/I_G ratio slightly decreased from 0.88 to 0.86 as the ferrocene to biochar ratio changed from 1:1–1:2. When the ratio was further increased from 1:2–1:3, the I_D/I_G ratio rose to 0.92. This increase in the I_D/I_G ratio for RHCNT 300 1:3 is possibly attributed to the presence of amorphous silica in rice husk biochar pyrolyzed at 300°C, which aligns with the findings of the XRD analysis discussed in 3.2. The results suggest that higher pyrolysis temperatures, along with a higher ferrocene to biochar ratio (e.g., 500°C and 1:3), improve the quality of the carbon nanotubes, yielding a higher degree of wall graphitization. The I_D/I_G ratios for each rice husk carbon nanotube sample are as follows: For RHCNT 500 1:1, the I_D/I_G ratio was 0.84; for RHCNT 500 1:2, it was 0.81; for RHCNT 500 1:3, it was 0.75. For RHCNT 400 1:1, the I_D/I_G ratio was 0.87; for RHCNT 400 1:2, it was 0.85; for RHCNT 400 1:3, it was 0.83. For RHCNT 300 1:1, the I_D/I_G ratio was 0.88; for RHCNT 300 1:2, it was 0.86; and for RHCNT 300 1:3, it was 0.92.

3.7. Field Emission Scanning Electron Microscopy (FESEM)

FESEM analysis is an effective method to visualize the surface topography of materials. Fig. 6**(a)–(f)** shows the surface morphology of RHCNT 500 and RHCNT 400, which showed elongated, tubular, and entangled structures. The surface morphologies of RHCNT 500 and RHCNT 400 showed close similarity to those ofommercially synthesized multi-walled carbon nanotubes (Kumar et al., 2015). The average diameter of RHCNT 500 1:1, RHCNT 500 1:2, RHCNT 500 1:3, RHCNT 400 1:1, RHCNT 400 1:2, and RHCNT 400 1:3 was 55 nm, 64 nm, 61 nm, 71 nm, 76 nm, and 78 nm, respectively. As the proportion of the carbon source (here, rice husk biochar) increases, the diameter of the synthesized carbon nanotubes decreases. RHCNT 500 1:1 was found to have the lowest diameter, followed by RHCNT 500 1:2 and RHCNT 500 1:3. Also, similar results were observed for RHCNT pyrolyzed at 400ºC, as RHCNT 400 1:1 had the lowest diameter compared to RHCNT 1:2 and RHCNT 1:3. The increase in diameter of carbon nanotubes at a 1:3 ferrocene to biochar ratio can be attributed to an insufficient amount of iron (Fe) nanoparticle catalysts (As they are liberated when ferrocene is decomposed at higher temperatures) for accommodating and synthesizing rice husk carbon nanotubes. Adequate amounts of iron nanoparticles are required for the self-assembly of carbon nanotubes. In agreement with this result, (Thonganantakul et al., 2018) pointed out that the equal weight proportion of ferrocene and carbon source (kerosene) yielded a carbon nanotube with lowest diameter. On the other hand, the surface morphology of RHCNT 300 1:1, RHCNT 300 1:2, and RHCNT 300 1:3 showed spherical, agglomerated structures (Fig. 6 **(g)-(i)**). Short tubular CNT structures were observed in all three rice husk carbon nanotubes pyrolyzed at 300ºC. For Rice husk CNTs pyrolyzed at 300ºC, the nucleation process of carbon nanotube growth was initiated, but further carbon nanotube synthesis was impeded by the presence of amorphous carbon and silica in Rice husk biochar pyrolyzed at 300ºC. Also, at higher pyrolysis temperatures of 400 and 500ºC, it can be concluded that amorphous carbon and silica became more crystalline, while carbon nanotube growth was not affected. As explained earlier in this work in 3.2, the degree of crystallinity of rice husk biochar increases with higher pyrolysis temperature. The average diameter of RHCNT 300 1:1, RHCNT 300 1:2, and RHCNT 300 1:3 was 98 nm, 102 nm, and 108 nm, respectively.

3.8. TEM analysis

TEM analysis provides information of internal structure of materials and it is crucial in characterizing CNTs. Fig. 7(a) depicts TEM image of RHCNT 500 1:1. They exhibited elongated, tubular structure similar to that of MWCNTs. Using ImageJ software, the length of synthesized RHCNT 500 1:1 was found to be in range of 1.09–1.43 μ. As observed in Fig. 7(b), the Iron NPs decomposed from ferrocene catalyst has encapsulated inside the tubular structure of CNT, possibly due to capillarity effect (Hidalgo et al., 2019). Under microwave irradiation conditions,

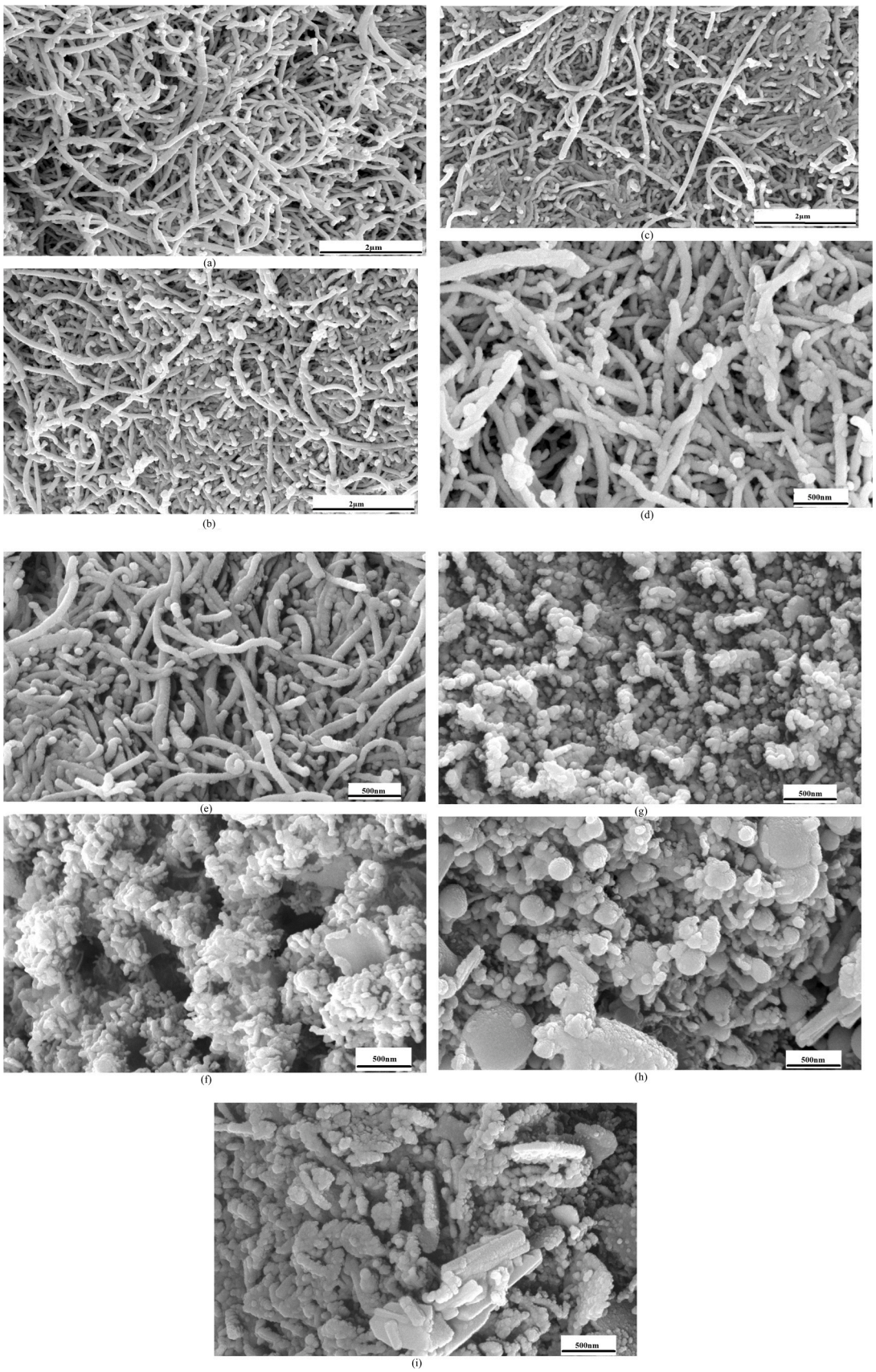

Fig. 6. FESEM images depicting surface morphology of (a) RHCNT 500 1:1, (b) RHCNT 500 1:2, (c) RHCNT 500 1:3, (d) RHCNT 400 1:1, (e) RHCNT 400 1:2, (f) RHCNT 400 1:3, (g) RHCNT 300 1:1, (h) RHCNT 300 1:2, and (i) RHCNT 300 1:3.

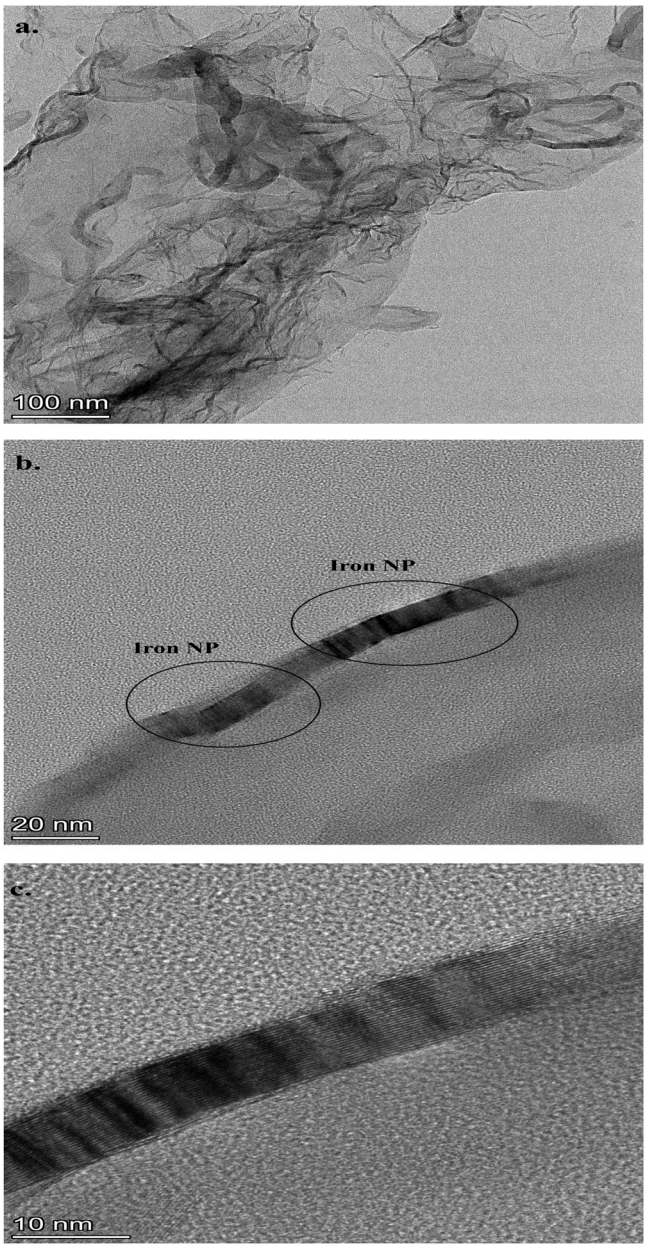

Fig. 7. a) TEM image of RHCNT 500 1:1, b) Encapsulated Iron NPs, c) Wall thickness of RHCNTs.

ferrocene decomposes into Fe atoms and cyclopentadienyl (Baghel and Kaushal, 2022). Upon further condensation and aggregation, iron atoms are converted into iron NPs. Further, iron NPs scattered on the surface of biochar reacts under microwave irradiation conditions to produce CNTs. Also, Fig. 7(c) shows the multiple layers of graphene sheets stacked one above the other in case of RHCNT 500 1:1, similar to that of MWCNTs. The average wall thickness of RHCNT 500 1:1 was calculated as 8.77 ± 0.46 nm using ImageJ software. Finally, RHCNT 500 1:1 exhibited 24–28 concentric walls, similar to those of Multi-walled carbon nanotubes (Roslan et al., 2019).

3.9. Yield of synthesized RHCNTs

The yield of synthesized RHCNTs is shown in Fig. 8. The highest and lowest yield of 0.34 ± 0.02 (gCNT/gRHBC) and 0.18 ± 0.01 (gCNT/gRHBC) was observed for RHCNT 500 1:1 and RHCNT 300 1:3, respectively. The CNT yield of synthesized RHCNT 500 1:2, RHCNT 500 1:3, RHCNT 400 1:1, RHCNT 400 1:2, RHCNT 400 1:3, RHCNT 300 1:1 and RHCNT 300 1:2 was 0.30 ± 0.01 (gCNT/gRHBC), 0.31 ± 0.01 (gCNT/gRHBC), 0.28 ± 0.02 (gCNT/gRHBC), 0.26 ± 0.02 (gCNT/gRHBC), 0.24 ± 0.02 (gCNT/gRHBC), 0.22 ± 0.01 (gCNT/gRHBC) and 0.19 ± 0.01 (gCNT/gRHBC), respectively.

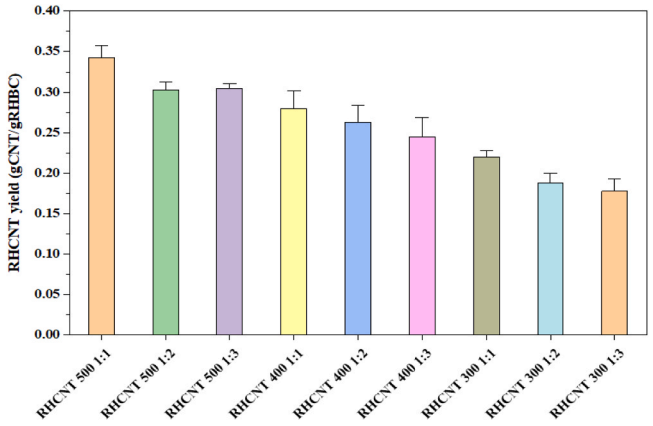

Fig. 8. Yield of synthesized RHCNTs.

The CNTs synthesized from biochar precursors pyrolyzed at higher temperatures gave higher yields. The RHBC produced at higher pyrolysis temperatures often has higher fixed carbon, as depicted in Table 1 of the Ultimate analysis, which ultimately increases the CNT yield. A similar observation was made by (Moothi et al., 2012), who reported higher CNT yield with increasing carbon content of precursor for CNT synthesis. Also, as the ferrocene to biochar ratio was increased, there was a decrease in CNT yield. As biochar content increases, there will be insufficient ferrocene catalyst to convert carbon precursors to CNTs, ultimately reducing yield. Egbosiuba et al. (2023) reported about 30 % of CNT yield by electric arc discharge method. CVD method exhibited a wide range of CNT yield from approximately 27–90 % with yield directly by synthesis temperature, carbon source, gas flow rates and catalysts type (Shukrullah et al., 2019). In summary, yield of RHCNT synthesis from two-step process is influenced by slow-pyrolysis temperature of rice husk and ferrocene to biochar ratio.

3.10. Energy analysis of the RHCNT synthesis process

The energy consumption of the RHCNT process is divided into four sections, namely, pre-treatment of biochar precursor, slow-pyrolysis of rice husk, microwave assisted synthesis of RHBC and finally post-treatment of the synthesized RHCNTs. As the rice husk samples were locally sourced, the energy consumed during transportation is not considered. In the pre-treatment phase, the open-air-dried samples are pulverized using a 750 W electric mixer for 20 min. The following equation gives the energy produced during pyrolysis of rice husk:

$$\text{Energy Input (KJ)}, E_{in} = Q_s + Q_{HHV} \quad (4)$$

Where, Q_s is the energy required to heat and transform feedstock into pyrolysis products and it is calculated by Eq. 5. The specific heat capacity of rice husk is taken as 1.67KJ/kgK (Hasan et al., 2024).

$$Q_s = m_{feed} * c_p * (T_P - T_{amb}) \quad (5)$$

Also, m_{feed} is the mass of the feedstock (kg), c_p is the specific heat capacity (KJ/KgK), T_P is the pyrolysis temperature, and T_{amb} is the ambient atmospheric conditions. Additionally, Q_{HHV} is the energy contained in the solid biomass, and it is given by the following relationship (Hasan et al., 2024):

$$Q_{HHV} = m_{feed} * HHV \quad (6)$$

HHV is the Higher Heating Value of the feedstock in KJ/Kg, and it is

given by the following equation (Parikh et al., 2005):

$$HHV(MJ/kg) = 0.3536*FC + 0.1559*VM - 0.0078*AC \quad (7)$$

Where FC is Fixed Carbon(%wt.), VM is Volatile matter(%wt.), and AC is ash content(%wt.), and it is obtained from the Ultimate analysis values as depicted in Table 1. During the CNT synthesis phase, a 900 W microwave oven is used for 15 min. Post-treatment involves initial sonication for 30 min in a 500-W sonicator, followed by drying the RHCNTs in a 1000-W electric oven for 30 min. The energy consumed by electrical equipment is calculated as the product of its power rating and its time of operation. The energy consumption per gram of RHCNT 500, RHCNT 400, and RHCNT 300 was separately calculated. The biochar and CNT yields were taken from the data in 2.1 and Fig. 8, respectively. A breakdown of the energy consumption of RHCNT 500, RHCNT 400, and RHCNT 300 is shown in Fig. 9. Total energy consumption ranged from 1.437 to 1.456 KWh, per gram of synthesized RGHCNTs. (Teah et al., 2020) conducted a LCA study on CNT synthesis using a fixed-bed and fluidized-bed CVD reactor. The cumulative energy demand per 1 g of CNT synthesis was estimated to be 408.71 MJ and 6.55 MJ for fixed-bed CVD and fluidized-bed CVD, respectively. The LCA study conducted by Khanna et al. (2008) revealed a cumilative energy demand (per 1 g of CNT produced) of 10.925MJ and 7.968MJ using methane and acetylene precursors, respectively. Additionally, Heidari and Younesi (2020) calculated the energy demand of 3.7–6.5MJ for CNT syntheses by waste tyre precursors using CVD method. In summary, the energy consumption for RHCNT synthesis at lab scale was found to be comparable to, and in some cases lower than, that of conventional CNT synthesis methods.

4. Conclusions

The present study focused on the synthesis of carbon nanotubes (CNTs) using rice husk biochar as a precursor. Based on the experimental results and analyses, the following key conclusions can be drawn:

- Rice husk CNT 500 and Rice husk CNT 400 exhibited elongated, tubular structures with average diameters between 55 and 71 nm, consistent with diameters of Multi-walled carbon nanotubes (MWCNTs), while Rice husk CNT 300 showed spherical, short-tubular structures due to incomplete growth caused by amorphous carbon and silica.
- Higher pyrolysis temperatures (400°C and 500°C) enhanced CNT growth by crystallizing amorphous carbon and silica, whereas pyrolysis at 300°C resulted in limited growth and retained amorphous phases, negatively affecting the structural integrity.
- Increasing the ferrocene-to-biochar ratio from 1:1–1:3 resulted in larger CNT diameters across all pyrolysis temperatures, with the highest wall graphitization and CNT quality observed for RHCNT 500 1:3.
- Raman spectroscopy revealed an I_D/I_G ratio below unity for all synthesized CNTs, indicating a high degree of graphitization, with the lowest ID/IG ratio observed for RHCNT 500 1:3, indicating the best graphitic quality.
- The maximum absorbance of rice husk CNT samples was observed between 208 and 226 nm, aligning with values reported in previous studies, confirming the optical properties of the synthesized CNTs.
- XRD analysis showed the presence of amorphous silica in Rice husk CNT 300 samples, leading to a broad peak at 22° that reduced the sharpness of the graphitic (002) peak, while higher temperatures improved crystallinity and graphitization.
- The study highlights rice husk biochar pyrolyzed at 400°C and 500°C, particularly at a 1:3 ferrocene-to-biochar ratio, as a sustainable and effective precursor for synthesizing CNTs with a favourable ID/IG ratio and an average diameter of < 100 nm, indicating good quality.

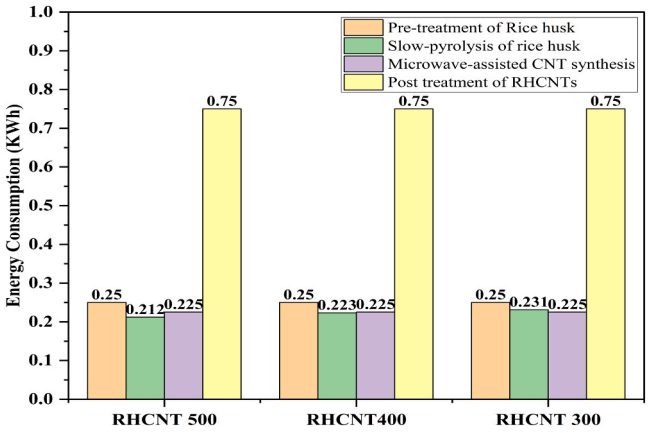

Fig. 9. Energy consumption of synthesized RHCNTs.

This study highlights the need for further research to establish clear screening criteria for selecting lignocellulose biomass precursors for microwave-assisted carbon nanotube synthesis and to understand better their influence on surface morphology, particle size, wall graphitization, wall thickness, inter-planar spacing, crystallinity, and yield. Investigating environmentally friendly liquid precursors, such as edible/non-edible oils, animal fats, and microalgae oils, for CNT synthesis offers a promising avenue. The potential of CNTs synthesized from biomass could address solid waste disposal issues and create value-added products. Also, post-synthesis treatments are crucial to address impurities and structural defects, enhancing CNT quality and expanding industrial applications are the expected future potentials of the study.

CRediT authorship contribution statement

Sai Parameshwar: Writing – original draft, Software, Methodology, Investigation, Formal analysis, Conceptualization, Data curation, Visualization. **Siddharth Jain:** Writing – review & editing, Supervision, Project administration, Methodology, Investigation, Funding acquisition, Formal analysis, Conceptualization, Resources, Software, Validation, Visualization. **Uday Bhan:** Writing – review & editing, Supervision, Methodology, Investigation, Conceptualization, Funding acquisition, Project administration, Resources, Software, Validation, Visualization. **Singh Dr Varun Pratap:** Writing – review & editing, Supervision, Formal analysis.

Funding

This work received financial support from the “Starting Research grant, Science and Engineering Research Board, Department of Science and Technology, India, under grant no. “SRG/2023/001949”.

Declaration of Competing Interest

The authors declare the following financial interests/personal relationships which may be considered as potential competing interests: Dr. Siddharth Jain reports financial support was provided by Science and Engineering Research Board. If there are other authors, they declare that they have no known competing financial interests or personal relationships that could have appeared to influence the work reported in this paper.

Acknowledgments

The authors would like to express their sincere gratitude to the Department of Petroleum Engineering and the Department of Mechanical Engineering, UPES, Dehradun, India, and the Solar Thermal Energy

Research Group, Stellenbosch University, South Africa, for their valuable contributions to this research. Their support and collaboration were instrumental in the successful completion of this study.

Data availability

Data will be made available on request.

References

Algadri, N.A., Hassan, Z., Ibrahim, K., Bououdina, M., 2017. Effect of ferrocene catalyst particle size on structural and morphological characteristics of carbon nanotubes grown by microwave oven. J. Mater. Sci. 52 (21), 12772–12782. https://doi.org/10.1007/s10853-017-1381-2.

Anzar, N., Hasan, R., Tyagi, M., Yadav, N., Narang, J., 2020. Carbon nanotube - A review on Synthesis, Properties and plethora of applications in the field of biomedical science. Sens. Int. 1, 100003. https://doi.org/10.1016/j.sintl.2020.100003.

Armynah, B., Atika, Djafar, Z., Piarah, W.H., Tahir, D., 2018. Analysis of chemical and physical properties of biochar from rice husk biomass. J. Phys. Conf. Ser. 979, 012038. https://doi.org/10.1088/1742-6596/979/1/012038.

Baghel, P., Kaushal, P., 2022. Rapid synthesis of carbon nanotubes from ProsopisJuliflorabiochar using microwave irradiation. Materials Science Engineering B 286, 115987. https://doi.org/10.1016/j.mseb.2022.115987.

Bajpai, R., Wagner, H.D., 2015. Fast growth of carbon nanotubes using a microwave oven. Carbon 82, 327–336. https://doi.org/10.1016/j.carbon.2014.10.077.

Burachevskaya, M., Minkina, T., Bauer, T., Lobzenko, I., Fedorenko, A., Mazarji, M., Sushkova, S., Mandzhieva, S., Nazarenko, A., Butova, V., Wong, M.H., Rajput, V.D., 2023. Fabrication of biochar derived from different types of feedstocks as an efficient adsorbent for soil heavy metal removal. Sci. Rep. 13 (1), 2020. https://doi.org/10.1038/s41598-023-27638-9.

Chen, Y., Zhang, X.-F., Wang, A.-J., Zhang, Q.-L., Huang, H., Feng, J.-J., 2019. Ultrafine Fe3C nanoparticles embedded in N-doped graphitic carbon sheets for simultaneous determination of ascorbic acid, dopamine, uric acid and xanthine. Microchim. Acta 186 (9), 660. https://doi.org/10.1007/s00604-019-3769-y.

Collins, P.G., Arnold, M.S., Avouris, P., 2001. Engineering Carbon Nanotubes and Nanotube Circuits Using Electrical Breakdown. Science 292 (5517), 706–709. https://doi.org/10.1126/science.1058782.

Divyabharathi, R., B., Kalidasan, J.S., Sakthi Surya Raj, Chinnasamy, S., 2024. Recent advances in sustainable agro residue utilisation, barriers and remediation for environmental management: Present insights and future challenges. Ind. Crops Prod. 216, 118790. https://doi.org/10.1016/j.indcrop.2024.118790.

Egbosiuba, T.C., Ani, I.J., Okafor, B.O., Mustapha, S., Tijani, J.O., Igwegbe, C.A., Okoye, C.C., Ulakpa, W.C., Ezennajiego, E.E., Abdulkareem, A.S., 2023. Carbon nanotubes–based nanoadsorbents in wastewater treatment. Adsorption through Advanced Nanoscale Materials. Elsevier, pp. 103–141. https://doi.org/10.1016/B978-0-443-18456-7.00006-7.

EsoheOmoriyekomwan, J., Tahmasebi, A., Zhang, J., Yu, J., 2022. Synthesis of super-long carbon nanotubes from cellulosic biomass under microwave radiation. Nanomaterials 12 (5), 737. https://doi.org/10.3390/nano12050737.

Hasan, M.M., Rasul, M.G., Jahirul, M.I., Mofijur, M., 2024. Fuelling the future: unleashing energy and exergy efficiency from municipal green waste pyrolysis. Fuel 357, 129815. https://doi.org/10.1016/j.fuel.2023.129815.

Heidari, A., Younesi, H., 2020. Synthesis, characterization and life cycle assessment of carbon nanospheres from waste tires pyrolysis over ferrocene catalyst. J. Environ. Chem. Eng. 8 (2), 103669. https://doi.org/10.1016/j.jece.2020.103669.

Hidalgo, P., Navia, R., Hunter, R., Coronado, G., Gonzalez, M., 2019. Synthesis of carbon nanotubes using biochar as precursor material under microwave irradiation. J. Environ. Manag. 244, 83–91. https://doi.org/10.1016/j.jenvman.2019.03.082.

Hidalgo, P., Navia, R., Hunter, R., Camus, C., Buschmann, A., Echeverria, A., 2023. Carbon nanotube production from algal biochar using microwave irradiation technology. J. Anal. Appl. Pyrolysis 172, 106017. https://doi.org/10.1016/j.jaap.2023.106017.

Hossain, M.M., Shima, H., Islam, Md.A., Hasan, M., Lee, M., 2016. Synergetic Effect in Raman Scattering of ZnO Nanoparticles in ZnO–CNT Fibers: A Way To Enhance the G and 2D Band. J. Phys. Chem. C. 120 (31), 17670–17682. https://doi.org/10.1021/acs.jpcc.6b03484.

Ighalo, J.O., Iwuchukwu, F.U., Eyankware, O.E., Iwuozor, K.O., Olotu, K., Bright, O.C., Igwegbe, C.A., 2022. Flash pyrolysis of biomass: a review of recent advances. Clean. Technol. Environ. Policy 24 (8), 2349–2363. https://doi.org/10.1007/s10098-022-02339-5.

Islam, T., Peng, C., Ali, I., Li, J., Khan, Z.M., Sultan, M., Naz, I., 2021. Synthesis of Rice Husk-Derived Magnetic Biochar Through Liquefaction to Adsorb Anionic and Cationic Dyes from Aqueous Solutions. Arab. J. Sci. Eng. 46 (1), 233–246. https://doi.org/10.1007/s13369-020-04537-z.

Khanna, V., Bakshi, B.R., Lee, L.J., 2008. Carbon nanofiber production. J. Ind. Ecol. 12 (3), 394–410. https://doi.org/10.1111/j.1530-9290.2008.00052.x.

Kharissova, O.V., Kharisov, B.I., 2014. Variations of interlayer spacing in carbon nanotubes. RSC Adv. 4 (58), 30807–30815. https://doi.org/10.1039/C4RA04201H.

Kim, A., Lim, S., Peck, D.-H., Kim, S.-K., Lee, B., Jung, D., 2012. Preparation and Characteristics of SiOx Coated Carbon Nanotubes with High Surface Area. Nanomaterials 2 (2), 206–216. https://doi.org/10.3390/nano2020206.

Kordi, M., Farrokhi, N., Pech-Canul, M.I., Ahmadikhah, A., 2024. Rice Husk at a Glance: From Agro-Industrial to Modern Applications. Rice Sci. 31 (1), 14–32. https://doi.org/10.1016/j.rsci.2023.08.005.

Kumar, A., Gupta, A., Sharma, K.V., 2015. "Thermal and mechanical properties of urea-formaldehyde (UF) resin combined with multi-walled carbon nanotubes (MWCNT) as nanofiller and fiberboards prepared by UF-MWCNT (Available at:). Holzforschung 69 (2), 199–205. https://doi.org/10.1515/hf-2014-0038.

Kumar, A., Kuang, Y., Liang, Z., Sun, X., 2020. Microwave chemistry, recent advancements, and eco-friendly microwave-assisted synthesis of nanoarchitectures and their applications: a review. Mater. Today Nano 11, 100076. https://doi.org/10.1016/j.mtnano.2020.100076.

Le, G.T.T., Mala, P., Ratchahat, S., Charinpanitkul, T., 2021. Bio-based production of carbon nanotubes via co-pyrolysis of eucalyptus oil and ferrocene. J. Anal. Appl. Pyrolysis 158, 105257. https://doi.org/10.1016/j.jaap.2021.105257.

Liu, L., Fu, S., Lv, X., Yue, L., Fan, L., Yu, H., Gao, X., Zhu, W., Zhang, W., Li, X., Zhu, W., 2020. A Gas Sensor With Fe2O3 Nanospheres Based on Trimethylamine Detection for the Rapid Assessment of Spoilage Degree in Fish. Front. Bioeng. Biotechnol. 8. https://doi.org/10.3389/fbioe.2020.567584.

Mao, Y., Robinson, J., Binner, E., 2021. Understanding heat and mass transfer processes during microwave-assisted and conventional solvent extraction. Chem. Eng. Sci. 233, 116418. https://doi.org/10.1016/j.ces.2020.116418.

Moothi, K., Iyuke, S.E., Meyyappan, M., Falcon, R., 2012. Coal as a carbon source for carbon nanotube synthesis. Carbon 50 (8), 2679–2690. https://doi.org/10.1016/j.carbon.2012.02.048.

Murjani, B.O., Kadu, P.S., Bansod, M., Vaidya, S.S., Yadav, M.D., 2022. Carbon nanotubes in biomedical applications: current status, promises, and challenges. Carbon Lett. 32 (5), 1207–1226. https://doi.org/10.1007/s42823-022-00364-4.

Namikuchi, E.A., Gaspar, R.D.L., da Silva, D.S., Raimundo, I.M., Mazali, I.O., 2021. PEG size effect and its interaction with Fe_3O_4 nanoparticles synthesized by solvothermal method: morphology and effect of pH on the stability. Nano Express 2 (2), 020022. https://doi.org/10.1088/2632-959X/ac0596.

Norizan, M.N., Moklis, M.H., Ngah Demon, S.Z., Halim, N.A., Samsuri, A., Mohamad, I.S., Knight, V.F., Abdullah, N., 2020. Carbon nanotubes: functionalisation and their application in chemical sensors. RSC Adv. 10 (71), 43704–43732. https://doi.org/10.1039/D0RA09438B.

Palma, V., Barba, D., Cortese, M., Martino, M., Renda, S., Meloni, E., 2020. Microwaves and heterogeneous catalysis: a review on selected catalytic processes. Catalysts 10 (2), 246. https://doi.org/10.3390/catal10020246.

Parikh, J., Channiwala, S., Ghosal, G., 2005. A correlation for calculating HHV from proximate analysis of solid fuels. Fuel 84 (5), 487–494. https://doi.org/10.1016/j.fuel.2004.10.010.

Pielsticker, S., Gövert, B., Umeki, K., Kneer, R., 2021. Flash Pyrolysis Kinetics of Extracted Lignocellulosic Biomass Components. Front. Energy Res. 9. https://doi.org/10.3389/fenrg.2021.737011.

Pode, R., 2016. Potential applications of rice husk ash waste from rice husk biomass power plant. Renew. Sustain. Energy Rev. 53, 1468–1485. https://doi.org/10.1016/j.rser.2015.09.051.

Quispe, I., Navia, R., Kahhat, R., 2017. Energy potential from rice husk through direct combustion and fast pyrolysis: A review. Waste Manag. 59, 200–210. https://doi.org/10.1016/j.wasman.2016.10.001.

Ranguwal, S., Sidana, B.K., Singh, J., Sachdeva, J., Kumar, S., Sharma, R.K., Dhillon, J., 2023. Quantifying the energy use efficiency and greenhouse gas emissions in Punjab (India) agriculture. Energy Nexus 11, 100238. https://doi.org/10.1016/j.nexus.2023.100238.

Rao, N., Singh, R., Bashambu, L., 2021. Carbon-based nanomaterials: synthesis and prospective applications. Mater. Today. Proc. 44, 608–614. https://doi.org/10.1016/j.matpr.2020.10.593.

Rathinavel, S., Priyadharshini, K., Panda, D., 2021. A review on carbon nanotube: An overview of synthesis, properties, functionalization, characterization, and the application. Materials Science Engineering B 268, 115095. https://doi.org/10.1016/j.mseb.2021.115095.

Rifna, E.J., RatishRamanan, K., Mahendran, R., 2019. Emerging technology applications for improving seed germination. Trends Food Sci. Technol. 86, 95–108. https://doi.org/10.1016/j.tifs.2019.02.029.

Roslan, M.S., Chaudhary, K.T., Doylend, N., Agam, A., Kamarulzaman, R., Haider, Z., Mazalan, E., Ali, J., 2019. Growth of wall-controlled MWCNTs by magnetic field assisted arc discharge plasma. J. Saudi Chem. Soc. 23 (2), 171–181. https://doi.org/10.1016/j.jscs.2018.06.003.

Sekar, M., Mathimani, T., Alagumalai, A., Chi, N.T.L., Duc, P.A., Bhatia, S.K., Brindhadevi, K., Pugazhendhi, A., 2021. A review on the pyrolysis of algal biomass for biochar and bio-oil – Bottlenecks and scope. Fuel 283, 119190. https://doi.org/10.1016/j.fuel.2020.119190.

Shamsollahi, Z., Partovinia, A., 2019. Recent advances on pollutants removal by rice husk as a bio-based adsorbent: A critical review. J. Environ. Manag. 246, 314–323. https://doi.org/10.1016/j.jenvman.2019.05.145.

Shoukat, R., Khan, M.I., 2021. Carbon nanotubes: a review on properties, synthesis methods and applications in micro and nanotechnology. Microsyst. Technol. 27 (12), 4183–4192. https://doi.org/10.1007/s00542-021-05211-6.

Shukla, P., Sudhakar, A., Gautam, P.V., Mansuri, S.M., 2022. Engineering Interventions to Mitigate the Agricultural Waste in India. Agriculture, Environment and Sustainable Development. Springer International Publishing, pp. 119–135. https://doi.org/10.1007/978-3-031-10406-0_8.

Shukrullah, S., Naz, M.Y., Mohamed, N.M., Ibrahim, K.A., Ghaffar, A., AbdEl-Salam, N. M., 2019. Production of bundled CNTs by floating a compound catalyst in an atmospheric pressure horizontal CVD reactor. Results Phys. 12, 1163–1171. https://doi.org/10.1016/j.rinp.2019.01.001.

Singh, M., Goyal, M., Devlal, K., 2018. Size and shape effects on the band gap of semiconductor compound nanomaterials. J. Taibah Univ. Sci. 12 (4), 470–475. https://doi.org/10.1080/16583655.2018.1473946.
Teah, H.Y., Sato, T., Namiki, K., Asaka, M., Feng, K., Noda, S., 2020. Life cycle greenhouse gas emissions of long and pure carbon nanotubes synthesized via on-substrate and fluidized-bed chemical vapor deposition. ACS Sustain. Chem. Eng. 8 (4), 1730–1740. https://doi.org/10.1021/acssuschemeng.9b04542.
Thakur, D., Ramawat, N., Shyam, V., 2020. Agricultural Waste Produce: Utilization and Management. Sustainable Food Waste Management. Springer Singapore, pp. 227–240. https://doi.org/10.1007/978-981-15-8967-6_13.
Thonganantakul, O., Chaiwat, W., Srinives, S., Suttiponparnit, K., Charinapanitul, T., 2018. Effect of Preloaded Ferrocene in Co-pyrolysis of Kerosene/Ferrocene on CNT Synthesis. J. Jpn. Inst. Energy 97 (7), 180–185. https://doi.org/10.3775/jie.97.180.
Vivanco-Benavides, L.E., Martínez-González, C.L., Mercado-Zúñiga, C., Torres-Torres, C., 2022. Machine learning and materials informatics approaches in the analysis of physical properties of carbon nanotubes: a review. Comput. Mater. Sci. 201, 110939. https://doi.org/10.1016/j.commatsci.2021.110939.
Wei, Y., Li, Z., 2016. Measurement of d-spacing of crystalline samples with SAXS. Measurement 93, 473–479. https://doi.org/10.1016/j.measurement.2016.07.051.
Yahyazadeh, A., Nanda, S., Dalai, A.K., 2024. Carbon Nanotubes: A Review of Synthesis Methods and Applications. Reactions 5 (3), 429–451. https://doi.org/10.3390/reactions5030022.
Yang, W., Wang, G., Chen, J., 2023. Oxidation of Ceftazidime by Modified Rice Husk Biochar-Activated Persulfate. Water Air Soil Pollut. 234 (12), 741. https://doi.org/10.1007/s11270-023-06760-4.
Zha, Z., Wu, K., Ge, Z., Ma, Y., Zeng, M., Wu, Y., Tao, Y., Zhang, H., 2023. Effect of oxygen on thermal behaviors and kinetic characteristics of biomass during slow and flash pyrolysis processes. Combust. Flame 247, 112481. https://doi.org/10.1016/j.combustflame.2022.112481.

Mr. Sai Parameshwar is a PhD research scholar in the Mechanical Engineering Department at UPES, Dehradun, India. He has pursued his B.Tech. in mechanical engineering from the University of Kerala and a master's in petroleum engineering from the University of Pune. He had worked as an Assistant Professor at Aditya Engineering College, Kakinada, Andhra Pradesh, and he taught subjects such as Reservoir Engineering, Enhanced Oil Recovery, etc. Currently, his research areas include clean energy production, Biodiesel, and carbon nanotube synthesis and characterization. He is also focused on agricultural and food waste management, effectively converting it into value-added products with a focus on commercial applications.

Dr. Siddharth Jain is a Senior Associate Professor in the Mechanical Engineering Department at UPES, Dehradun, India. Dr. Jain's undergraduate training has been predominantly in mechanical engineering. He pursued his master's and doctoral degrees in Biomass and Bioenergy at the Indian Institute of Technology Roorkee, India. After his PhD, he earned his two Post-Doctoral Fellowships from the National University of Singapore and the University of Alberta in biomass and Bioenergy. Currently holding many research grants from the Government. of India in the field of waste management and utilization.

Dr. Uday Bhan has pursued his M. Sc. in Applied Geology from the University of Allahabad, India; an M. Tech in Petroleum Exploration from IIT, Dhanbad, India; and a PhD in Earth Science from the University of Petroleum & Energy Studies [UPES], Dehradun, India, in 2012. At present, Dr. Uday Bhan is a Professor & Program Lead in the Department of Petroleum Engineering & Earth Sciences at UPES. He is an active researcher in the following areas: hydrogeology, reservoir characterization, biodiesel-based drilling fluids, and atmospheric pollutants at high altitudes. He has published 60 + research papers in peer-reviewed journals, 12 book chapters in his research areas, and supervised 5 PhD students and 10 + UG & PG projects. DR. Uday Bhan is looking and keen to work on energy and multidisciplinary research.

Dr. Varun Pratap Singh is an Associate Professor (Extraordinary) at Solar Thermal Energy Research Group (STERG) at the University of Stellenbosch, South Africa, and an Assistant Professor-SG in the Department of Mechanical Engineering at UPES Dehradun, India. He received his B.Tech., M.Tech., and PhD degrees in Mechanical Engineering, specializing in solar thermal energy, from Uttar Pradesh Technical University and Uttarakhand Technical University, respectively. His research interests include the study and analysis of renewable energy, solar thermal systems, biofuels, micro-hydro turbines, green hydrogen, life-cycle assessment, and special-purpose machines with TRL 6 + applications.